Thermal desorption of cold positronium from oxygen-treated Al(111) surfaces

A. P. Mills, Jr., E. D. Shaw, M. Leventhal, R. J. Chichester, and D. M. Zuckerman
AT&T Bell Laboratories, Murray Hill, New Jersey 07974-0636
(Received 7 March 1991)

We have measured the yields and energy spectra of positronium (Ps) emitted from Al(111) surfaces treated by exposure to oxygen gas at low temperatures. We find that the oxygen induces the emission of Ps with kinetic energies of a few tenths of an eV, in agreement with previous work. We also find that Ps is thermally desorbed at low temperatures and has a velocity distribution characterized by a temperature that is the same as that of the sample. The intensity of the thermal Ps component is about 12% of the positrons that reach the surface. The velocity distributions may be interpreted as indicating that the Ps has a sticking coefficient of 1 in the limit of zero velocity, unlike any other system studied to date.

I. INTRODUCTION

Positronium, the e^+-e^- atom that may be formed by positrons picking up an electron from a variety of materials, was discovered by Deutsch[1] while observing the behavior of positrons in gases. In one of the first studies of the interactions of slow positrons with a solid surface, Canter, Mills, and Berko[2] found a high probability for the emission of free positronium (Ps) into the vacuum following positron bombardment of a metal target. Subsequent work[3] has shown that there are two mechanisms by which thermal positrons produce Ps in vacuum at a clean metal surface: a direct process that yields Ps with eV kinetic energies,[2,4,5] and a thermally activated process[4-7] that yields Ps with an energy distribution characteristic of the temperature of the solid surface.[5,8] The velocity spectrum of the Ps associated with the direct process yields information about the Ps formation mechanism[9-11] and the electronic properties of the near-surface region of the solid.[12-16] The thermally activated Ps is useful for making precise measurements of the atomic properties of Ps,[17] for measuring the binding energy of the positron surface state,[6,7,18-23] and for studying the surface interactions of slow Ps.[8,24]

In a typical experiment to study the surface interactions of a positron in near thermal equilibrium with a solid, positrons from a slow positron beam are implanted into a target surface prepared in ultrahigh vacuum. Implantation kinetic energies of several keV are needed to insure that the positrons stay in the solid long enough to become sufficiently thermalized.[25-27] In a good single crystal, the positron diffusion length L_+ is about 1000 Å, and the probability of a positron encountering the sample surface if it starts at a depth x is $\exp(-x/L_+)$. It has recently been discovered that low-energy positrons inside the solid exhibit quantum reflection from the surface potential so that the probability of their escape from the bulk at temperatures below ambient is proportional to $k_\perp$,[28] the component of the positron momentum in the solid that is perpendicular to the surface.

At the surface there are several channels for positron escape from the bulk solid.[3] The positrons may be emitted into the vacuum as bare particles if the positron work function of the solid is negative;[25] they may capture an electron and be ejected as Ps with an energy of a few eV depending on the Ps work function and the electronic density of states near the surface;[9] and they may be captured into a surface state that exists because of the image-correlation potential well seen by a positron just outside the solid. The surface positron state seems to be partly like a bare particle bound to the surface[29-31] by about 3 eV and partly like a Ps atom bound to the surface[32] by van der Waals forces with a binding energy E_a of order 0.5 eV. For most metals studied so far it is possible to desorb the surface positronium atoms into the vacuum by heating the solid. The desorbed positrons form Ps with a thermal energy distribution, and the yield of thermal Ps measured as a function of sample temperature may be used to estimate E_a.[6,7]

The aims of the present study were to find a stable and simply prepared surface that would emit slow Ps at low temperatures; to verify the existence of a thermal Ps component by measuring the energy distribution of the Ps; and to investigate the surface interactions of slow Ps by comparing the energy distributions with theory. Thus far, the thermal desorption of Ps from typical clean metal surfaces has required sample temperatures at or above room temperature. However, the activation energy E_a may be lowered by the influence of an adsorbed surface layer, suggesting the possibility of Ps desorption at low temperatures.[7,33] In the present study we make use of Lynn's discovery that submonolayer coverage of oxygen on Al surfaces causes an increase in the Ps yield.[34,35] We note that it is important to actually measure the energy spectra because a Ps yield that increases with temperature does not necessarily mean that we are forming Ps with a temperature characteristic of the sample. For example, the Ps emitted by graphite requires the presence of thermal phonons to conserve parallel momentum, even though the Ps has a negative affinity.[10] As a result, the Ps yield varies with temperature in a manner that might seem to suggest thermal desorption and the emission of thermal Ps, but the Ps kinetic energy is much greater than thermal energies. It also might be possible for the surface contamination to change with temperature, leading to a temperature dependence for the Ps yield. For ex-

ample, in the case of the oxygen on Al system, it is essential that the oxygen exposure occur at low temperature because above 300 K the physisorbed surface oxygen atoms migrate into the bulk.[34–37] The electronic density of states may thereby acquire a peak below E_F that causes the direct emission of Ps with kinetic energies much less than the usual negative work function Ps.[38] In making measurements of the energy spectra of thermally desorbed Ps it is thus important to maintain the sample temperature below 300 K and to properly subtract the component of the spectrum due to the directly emitted Ps.

II. EXPERIMENT

Our measurements were made using positrons generated by a microtron accelerator[39,40] in 7-nsec-wide pulses at 30 Hz containing 5×10^4 slow e^+ with kinetic energies at the target surface spread between 1.4 and 3.9 keV. The positrons are implanted into a 99.999%-pure Al(111) sample prepared by electropolishing in a 1:5 perchloric acid-ethanol mixture and by repeated cycles of Ar^+-ion bombardment and annealing at 820 K *in situ*. Auger spectroscopy before exposure to oxygen showed that the surfaces were initially contaminated by less than 1% of a monolayer of C and O.

The Ps energy distributions $dN/dE_\perp$ are measured by a time-of-flight method[5,41] using a sample and slit geometry similar to that of Ref. 42 and indicated in Fig. 1. Ps emitted from the sample surface with a given value of $E_\perp$ may be detected at time $t=\Delta z\sqrt{m_e/E_\perp}$ if it annihilates in front of the detector slit. Here, the distance from the sample surface to the center of the slit is Δz. The detector is an annular plastic scintillator (Bicron BC408) 5 mm thick, 200-mm inside diameter, and with a square outer perimeter, 400 mm on a side. The detector is coupled to two adiabatic light pipes viewed by two Hamamatsu H1949 (1828-01) photomultiplier tubes, the outputs of which were summed. In our geometry, a triplet Ps atom decaying into three photons at the center of the slit would be detected with a probability of about 2%. The full width at half maximum of the slit resolution function was measured (see Fig. 2) to be $\delta z=(1.8\pm0.2)$ mm.

To measure the effect of O_2 exposure on the low energy tail of the directly emitted Ps energy distribution, we have measured the Ps time of flight using a 10-mm flight path and an analysis of photographically recorded spectra. The sample was cleaned, cooled to 230 K, and exposed to various amounts of oxygen. The data were obtained by recording the output of the detector on a LeCroy 9450 digital oscilloscope that was triggered on the positron bunching-voltage pulse. The signals shown in Fig. 3 were averaged over 1000 positron pulses and recorded photographically. The preliminary runs allowed us to determine that 100 L (1 L $=10^{-6}$ Torr sec) of oxygen is too much for making slow Ps, and 5 L is too little, and thus set the scale for our more precise experiments described below.

We have examined in detail the effect of oxygen exposure and temperature, again using time of flight, but with a shorter flight path and digitally recorded data for more sensitivity to low energies. The data were obtained with the manipulator set to 319.0 mm. Since the centroid of the peak in Fig. 2 is at $z=(323.9\pm0.2)$ mm, the nominal flight distance was 4.9 ± 0.2 mm.

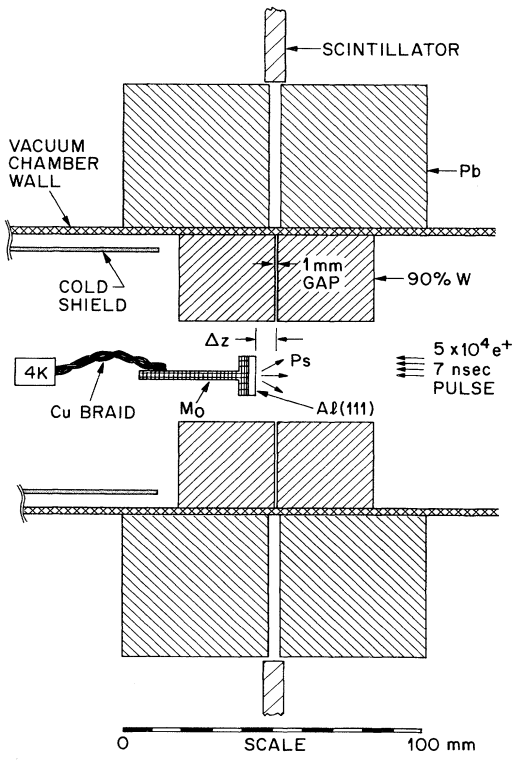

FIG. 1. Geometry of the target and detector slit.

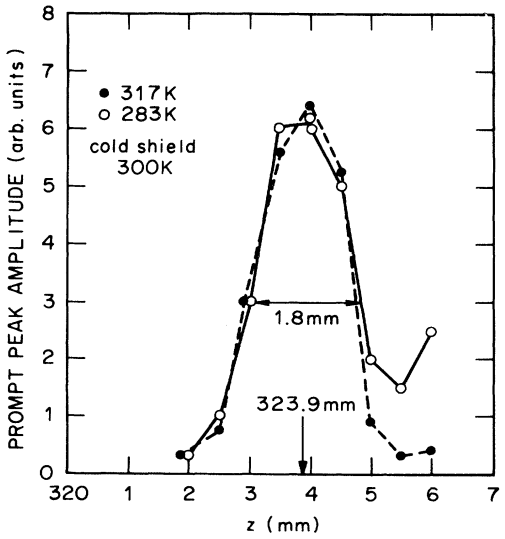

FIG. 2. Prompt peak amplitude as a function of sample manipulator position z.

There are a number of corrections that increase the nominal value of Δz. First, some of the events detected in Fig. 2 are due to singlet Ps annihilating about 0.1 mm in front of the sample surface, which causes the measured Δz to be too small by about 0.02 mm. Second, scattering of annihilation photons in the sample makes their distribution forward directed, making the measured Δz too small by about half a slit width, or 0.5 mm. Third, the manipulator shrinks during the measurements at low temperature by an average amount estimated to be about 0.4 mm. Finally, the time-of-flight distribution will be slightly lopsided because the slit width is not negligible, causing Δz to appear too small by roughly 0.05 mm. Applying the sum of these effects with a conservative error estimate leads to a corrected effective flight distance of $\Delta z = 6.0 \pm 0.5$ mm.

For our set of data on the dependence of the slow Ps emission of oxygen exposure, the sample was cooled to 186 K and then exposed to 1.6×10^{-8} Torr of O_2 for a period of 2 h, during which the time-of-flight spectra shown in the upper portion of Fig. 4 were recorded every five minutes. For display, the effect of o-Ps decay has been removed by multiplying the data by $\exp(+t/\tau)$, where τ is the 142-nsec lifetime of orthopositronium in vacuum. During the course of the run the temperature varied by less than ± 3 K. Correcting for the geometry of the vacuum chamber and the location of the leak valve, sample and pressure gauge, we estimate that the O_2 exposure rate was equivalent to 0.6 L/min ($1\ \mathrm{L} = 10^{-6}$ Torr sec at 300 K). The cold shield surrounding the sample manipulator was kept at room temperature during the oxygen exposure, since the shield when cold was a very effective pump and significantly reduced the oxygen pressure at the target.

For our set of data on the temperature dependence of the Ps emission, the sample was cooled to 205 ± 5 K and then exposed to 5×10^{-8} Torr of O_2 for 15 min. We estimate that the corrected O_2 exposure was equivalent to 24 L and resulting in roughly a one-third monolayer of O on the Al surface. We were unfortunately unable to obtain

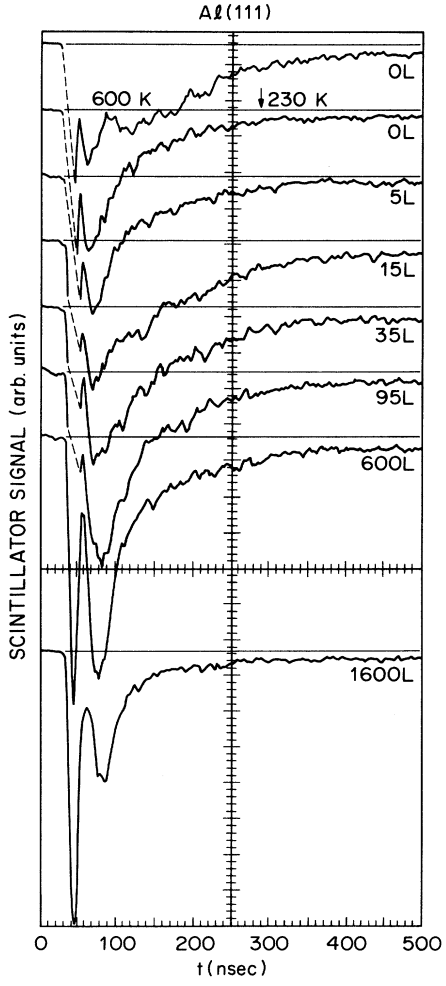

FIG. 3. Direct detector output recorded by a digital oscilloscope (LeCroy 9450, 2.5-nsec sample interval). Each trace is an average over 1000 events.

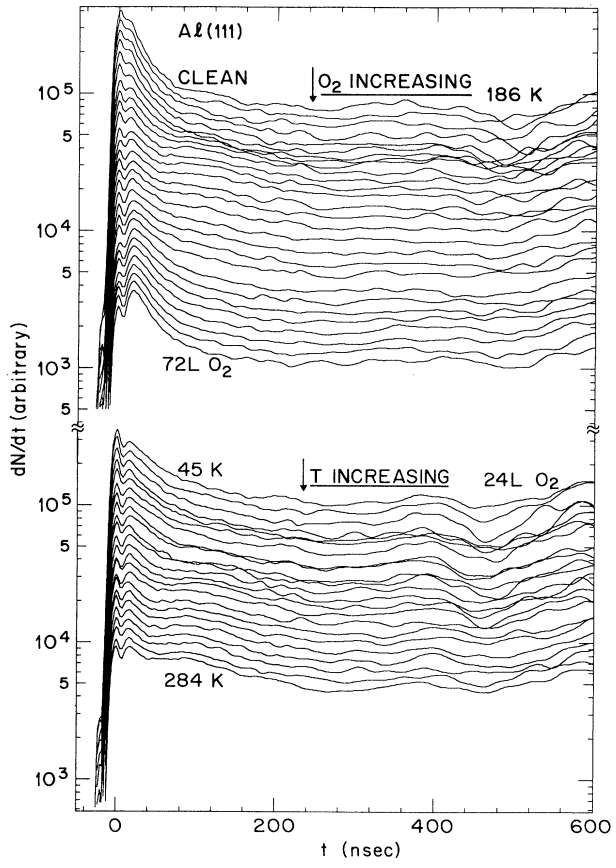

FIG. 4. Time spectra showing the effect of oxygen exposure at a fixed temperature of 186 K, and the effect of temperature for an oxygen exposure of 24 L. ($1\ \mathrm{L} \equiv 10^{-6}$ Torr sec.) The spectra have been multiplied by $\exp(t/\tau)$ to remove the effect of the orthopositronium decay, and have been smoothed somewhat at larger values of t.

meaningful Auger determinations of the oxygen concentrations apparently because of the effect of the Auger electron beam on the surface oxygen atoms. After the exposure the pressure in the vacuum chamber fell below 10^{-10} Torr in a few minutes, and below the limit of the gauge (3×10^{-11} Torr) about 30 min after starting to cool the cold shield surrounding the sample manipulator. Time-of-flight spectra were recorded every 2 min as the sample was cooled over the course of one hour to 45 K and then warmed for 30 min at a constant rate up to 284 K. The raw data are shown in the lower portion of Fig. 4.

III. RESULTS

The amplitudes of the photographically recorded time-of-flight data shown in Fig. 3 were measured with a ruler over the range 20–80 nsec after the prompt peak, which corresponds to Ps kinetic-energy components perpendicular to the surface $E_\perp$ in the range 0.1–1.8 eV. The amplitudes were converted to the spectra of the perpendicular component of the positronium energy $dN/dE_\perp$ shown in Fig. 5 by multiplying by $t^2\exp(+t/\tau)$ and plotting on an energy scale.

The curve corresponding to data obtained before exposure of the sample to oxygen (labeled "0 L") may be compared with the spectrum predicted by Eq. (2) of Ref. 9 for the Ps spectrum from a free-electron metal:

$$dN/dE_\perp \propto E_\perp^{1/2}\tan^2\alpha\,\theta(|\phi_{Ps}|\cos^2\alpha - E_\perp) + E_\perp^{-1/2}(|\phi_{Ps}| - E_\perp)\theta(|\phi_{Ps}| - E_\perp) \times\theta(E_\perp - |\phi_{Ps}|\cos^2\alpha)\ . \quad (1)$$

Here α is the collimator half angle, 60° in the present geometry, and $\theta(x)$ is the unit step function. The quantity ϕ_{Ps} is the positronium work function given by $\phi_{Ps}=\phi_+ + \phi_- - \frac{1}{2}R_\infty$, where ϕ_+ and ϕ_- are the positron and electron work functions, and $\frac{1}{2}R_\infty$ is the binding energy of Ps. Equation (1) predicts that $dN/dE_\perp$ will increase as $E_\perp^{1/2}$ for $E_\perp < \cos^2\alpha|\phi_{Ps}| = 0.6$ eV, and will then decrease slightly more rapidly then linearly to zero at $E_\perp = |\phi_{Ps}| = 2.5$ eV. The data agree with such a form above 0.6 eV, but as was found in Ref. 14, there is more intensity than expected at the very low energies, possibly due to a residual oxygen contamination, as was suggested in Ref. 14. Also, we find in agreement with Ref. 38 and with Howell, Tuomisaari, and Jean[43] that increasing oxygen exposure causes a large increase in the intensity of the low-energy component that, given the energy scale of tenths of an eV, has nothing to do with the emission of thermal Ps.

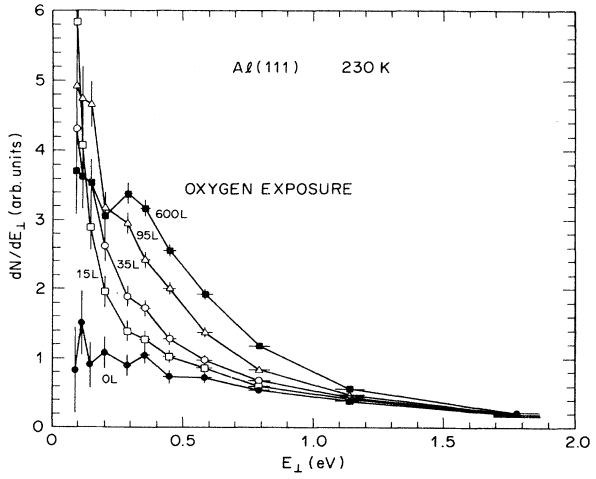

FIG. 5. Spectra of the perpendicular component of the Ps energy deduced from the data of Fig. 3.

The many individual spectra making up each trace in Fig. 4 were summed in real time on a computer that had much better amplitude resolution than the 9450 oscilloscope that recorded the average spectra of Fig. 3. The minimum useful intensity is limited by a small ringing of the base line (due to a ground loop) that becomes pronounced after about 400 nsec in Fig. 4. The effect is slightly different in different traces because of small changes in the position of signal wires during the run. The digitally recorded time-of-flight data were analyzed by calculating the amount of fast and slow positronium as follows. The data were first multiplied by $\exp(+t/\tau)$ to obtain $S(t)$, the time-of-flight data with the effect of o-Ps decay removed that is plotted in Fig. 4. A background given by the average value of $S(t)$ in the interval from 280 to 380 nsec was then subtracted from $S(t)$. The data were normalized to the sum of the three peak channels. The amount of Ps in a given time interval $a<t<b$ is proportional to the integral $A=\int_a^b S(t)dt/t$. The area of the slow component of the Ps, A_s, was computed for $52<t<240$ nsec corresponding to perpendicular energies $4<E_\perp<76$ meV, using 6 mm for the time-of-flight distance. The area of the fast component, A_f, was found by summing over the range $12.5<t<50$ nsec, which corresponds to energies 82 meV $<E_\perp<1.3$ eV. The fast-component area was multiplied by 1.2 to correct for the fast Ps not included in the summation, according to Eq. (1). Finally, the area corresponding to the total amount of Ps, $A_t=1.2A_f+A_s$, was normalized to cause the maximum Ps yield to be about 95%. The normalization appears to be reasonable since the Ps yield before oxygen exposure is then about 55%, in agreement with the known[7,8,18] 50–60% total Ps yield of clean Al(111) at room temperature.

The total amount of Ps and the "fast" and "slow" components as defined in the previous paragraph are plotted in Fig. 6 as a function of oxygen exposure, and in Fig. 7 as a function of temperature for the Al(111) surface after exposure to 24 L of oxygen. There are systematic errors in these two plots because of the uncertainty in our definitions of "fast" and "slow" and some arbitrariness in how we have attempted to remove the background. However, we do not expect such errors to obscure qualitative trends. Thus, from Fig. 6 we conclude that the "slow" Ps component for the initially clean Al(111) sample at 186 K reaches a maximum after an exposure of about 30 L, and that the fast component begins to increase for larger exposures. Similarly, we conclude from

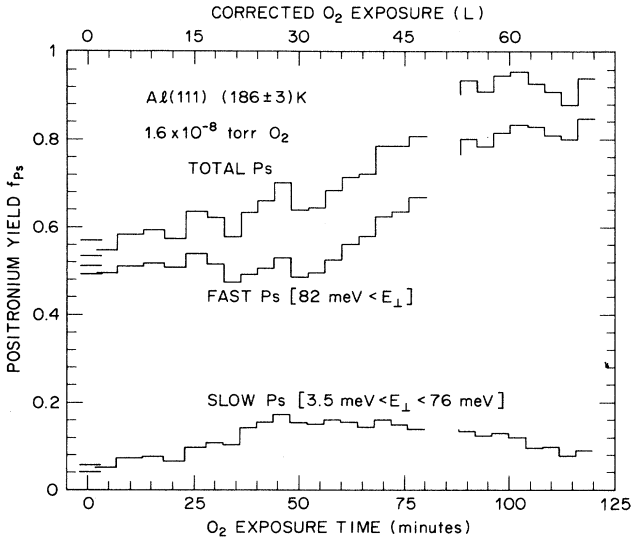

FIG. 6. Amount of "fast" positronium and "slow" positronium deduced from the oxygen-exposure series of spectra in Fig. 4 by integrating over time ranges corresponding to the energy intervals indicated. The normalization was chosen so that the total amount of positronium approaches unity at large oxygen exposures. The gap starting at 80-min exposure time was caused by the computer disc becoming full.

Fig. 7 that the "slow" Ps component for Al(111) after an oxygen exposure of 24 L increases with temperature, while the "fast" component changes only a little.

In the case of the temperature effect on the "slow" Ps component, we can obtain the actual spectrum of the changing part by subtracting a suitably normalized cold spectrum from each of the higher-temperature runs, assuming that the "fast" component is unaffected by temperature. The "cold" spectrum was taken to be the aver-

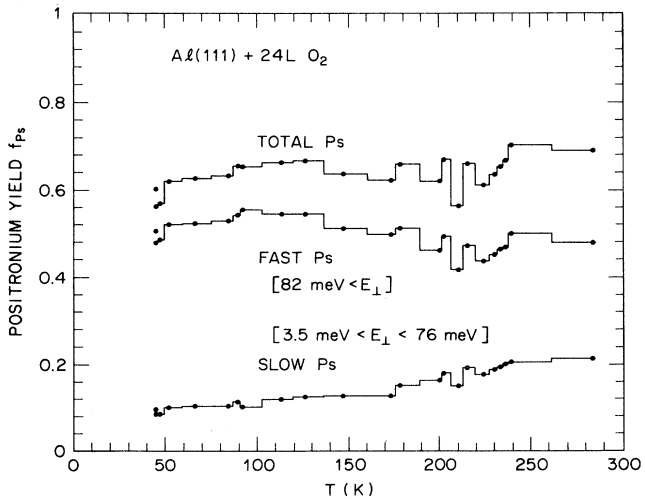

FIG. 7. Amount of "fast" positronium and "slow" positronium deduced from the temperature series of spectra in Fig. 4 by integrating over time ranges corresponding to the energy intervals indicated. The normalization is the same as in Fig. 6.

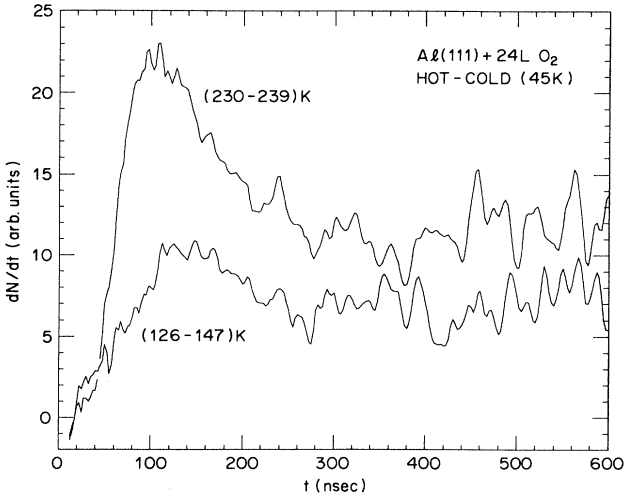

FIG. 8. Difference time-of-flight spectra for two sample temperatures.

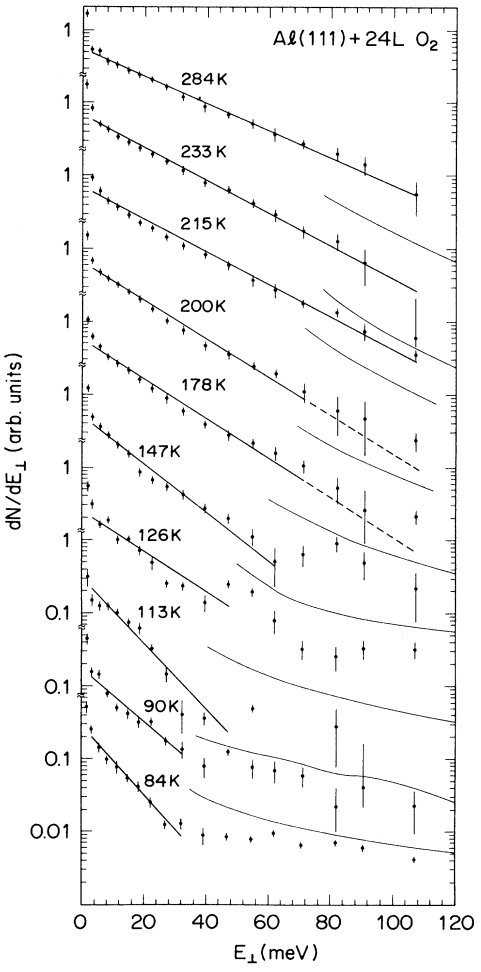

FIG. 9. Spectra of the perpendicular component of the energy of Ps thermally desorbed at various temperatures from an Al(111) surface exposed to 24×10^{-6} Torr sec of O_2. The solid lines are fitted exponential functions of $E_\perp$.

TABLE I. Results of fitting simple exponential curves to the Ps energy distributions shown in Fig. 9.

Run	Time of day (h:m)	Sample T[a] (K)	Ps kT[b] (meV)	Area (arb. units)	y^0	χ^2	ν
1	16:24	84±7	9.3±0.6	251	272	15.22	7
2	15:58/16:28	90±15	11.9±1.2	204	171	17.96	7
3	16:32	113±3	9.7±0.8	275	284	24.23	9
4	15:54	126±19	15.9±2.2	381	240	87.95	9
5	16:36	147±6	13.3±0.8	631	475	28.16	11
6	15:50	173±27	14.2±0.7	671	474	23.93	11
7	16:40	178±4	16.1±0.7	875	544	28.27	12
8	15:22	200±1	16.5±0.6	1047	636	18.39	12
9	16:44	202±4	17.9±0.7	1092	611	19.11	12
10	15:26	210±7	17.9±0.8	1092	701	37.93	15
11	15:46	215±8	19.5±0.7	1325	681	39.39	15
12	15:30	224±7	18.7±0.7	1273	682	23.82	15
13	15:42	230±1	20.7±0.8	1360	658	36.75	15
14	15:38	233±3	19.4±0.7	1290	666	18.64	15
15	15:34	236±2	20.7±0.8	1303	630	25.66	15
16	16:48	239±3	22.0±0.8	1226	557	32.77	15
17	16:52	284±4	23.1±0.6	1271	550	8.52	14

[a]The ± value gives the range of T during the measurement and does not represent the error assignment for the average value of T quoted.

[b]The values of kT for the Ps atoms were computed using 6.0 mm as the time-of-flight distance. The errors have been increased over the estimated statistical error by the square root of χ^2 over the number of degrees of freedom, ν.

age of three spectra taken at the coldest temperature, 45 K. Each higher-temperature spectrum was normalized to the "cold" spectrum by equating the areas in the intervals between 15 and 20 nsec after the prompt peak. After subtracting, the difference spectrum was multiplied by $\exp(t/\tau)$. Two examples of the difference time-of-flight spectra are shown in Fig. 8. The two curves are each averaged over three runs with temperatures in the ranges 230–239 and 126–147 K. The peaks of the time-of-flight difference spectra occur at 110 and 140 nsec, corresponding to $E_\perp = 17$ and 10 meV, respectively. The background due to 3γ decay of Ps not in sight of the slit appears as a constant. The background was taken to be the average over the interval from 25 to 35 nsec after the prompt peak and was subtracted. The resulting time-of-flight spectra were converted to energy spectra by multiplying by t^2 and plotting on an energy scale. Figure 9 displays ten of the energy spectra and fitted simple exponential curves. For sufficiently long time delays the data depart from the fitted curve due to the difficulty of determining the background accurately. The problem becomes more severe at the lower temperatures where the amplitude of the thermal Ps component is becoming weaker. Table I lists the fitting parameters for all the data. The Ps temperatures deduced from the energy spectra are plotted in Fig. 10. The total area of the curves fitted to all the thermal Ps spectra are plotted in Fig. 11 versus sample temperature. In addition to statistical uncertainties, the total areas under the curves are affected by the opposing temperature dependences of e^+ reflection and diffusion, the former[28] decreasing and the latter increasing the number of e^+ reaching the surface as the temperature is lowered. Taking into account the lack of thermalization of the implanted e^+, we estimate such effects produce a systematic shift in the areas roughly the size of the statistical errors. The fitted curves will be discussed below.

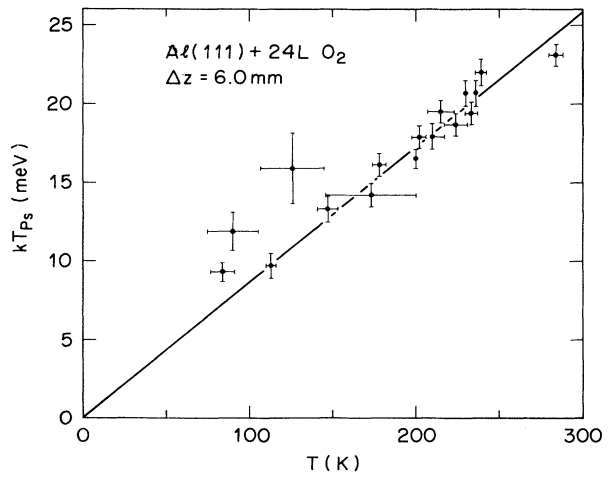

FIG. 10. Correlation of the fitted positronium temperature with the sample temperature for the data series corresponding to Figs. 7 and 9.

IV. DISCUSSION

A. Effect of oxygen on fast positronium

The first measurement[9] of the effect of oxygen on the energy spectrum of the direct Ps showed that a 100-L room-temperature exposure cut the intensity of the Ps at the maximum energy $-\phi_{Ps}$ in half, and possibly increased

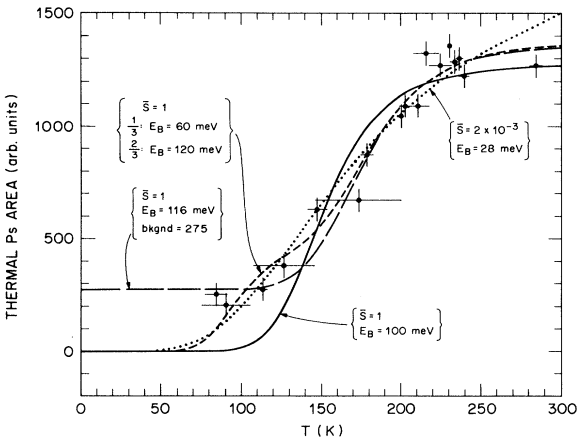

FIG. 11. Total amount of thermal Ps vs sample temperature. The thermal positronium yield is the area of the fitted exponential curves in the temperature series corresponding to Figs. 7, 9, and 10. The full scale yield corresponds to about 15% of the positrons that reach the surface.

the probability of emission of Ps with energies below 1.5 eV. An angle-resolved measurement of the Ps momentum distribution[14] confirmed the reduction of the maximum-energy Ps component and yielded a measurement of the spectrum associated with the addition of oxygen.[38] Quoting from Ref. 38, "The thin-oxide layer on the Al(111) surface produces a much narrower Ps spectrum with a most probable momentum of 1 mrad (i.e., a most probable energy of 130 meV)." The latter statement was referring to a 3×10^4 L oxygen exposure. A 150-L exposure of a Al(100) surface at 300 K, corresponding to about one monolayer coverage, yielded a most probable Ps energy of about 250 meV, in rough agreement with out 95-L measurement in Fig. 5. The decrease in energetic Ps upon oxygen exposure is in agreement with a density-of-states calculation, but the increase in the lower-energy Ps component does not appear to be in quantitative agreement with theory because the electronic density of states for the oxide peaks at 5–10 eV below the Fermi surface, and thus cannot participate in the Ps formation.[9,38,44–48]

An interesting resolution to the above difficulties of interpretation is offered by Howell, Tuomisaari, and Jean,[43] who have made a further study of the effect of oxygen on the Ps energy spectra from Al(111). They suggest that rather than the oxygen $2p$ metal bonding states, the positron is sensitive to oxygen *antibonding* states lying a few eV higher in energy. They also suggest that the Ps formation would be more sensitive to the antibonding states than photoemission because the states extend far into the vacuum, where the Ps formation is most likely.

B. Effect of oxygen on thermal positronium

We have seen from Fig. 6 that the slow Ps yield of Al(111) at 186 K increases with oxygen exposure to a maximum of about 12% at about 30 L. We have subtracted the "slow"-component yield of the clean Al (4%), which is only the low energy part of the directly emitted Ps energy distribution. At about 35 L the intensity of the "fast" Ps starts to increase. According to Chen, Crowell, and Yates,[37] "at very low oxygen exposure, oxygen dissociatively adsorbs to occupy both surface and subsurface binding sites without formation of the oxide . . . a critical number of oxygen atoms in both surface and subsurface adsorption sites must cluster in order to form aluminum oxide." The latter begins to form at about 40-L exposure for Al(111) at 135 K.[37] It would appear that the fast Ps is associated with the oxide formation, i.e., the appearance of Al^{3+}, and that the slow Ps is associated with the surface adsorption of oxygen. Such a conclusion is in agreement with Ref. 43, if one remembers that they were not sensitive to very-low-energy Ps. The small amount of slow Ps compared to the 50% yield of thermal Ps from clean Al(111) at 692 K (Ref. 8) may indicate that the positron surface state that is the source of the thermal Ps is less efficient at trapping positrons when there is oxygen present. The data of Ref. 43 appear to be in disagreement, but their sample was at 300 K. However, according to Erskine and Strong,[49] "the surface oxygen phase is unstable and converts at room temperature to subsurface oxygen." In fact, we have not been able to make cold Ps when we start from a room-temperature oxygen exposure, but this may have been due to undetected coincidental circumstances, such as failure to anneal the Al sample sufficiently. It is clear that the Al plus oxide system is not simple, and that further work to elucidate the Ps emission mechanisms must be done at low temperatures and in parallel with other spectroscopies such as electron-energy-loss spectroscopy (EELS), low-energy electron diffraction (LEED) and photoemission, as well as Auger. As an example, McConville *et al.*[50] and find that there are four different chemically shifted Al $2p$ photoemission peaks present for room-temperature exposures on the order of 100 L, and that water exposure gives different results from O_2.

C. Thermal desorption of positronium

If Ps on the surface is a free particle in two dimensions (2D) with a single well-defined binding energy E_B, and if all the excited states on the surface can be characterized by the temperature T, and if the density of e^+ in the bulk is low enough, then thermodynamics gives us the total desorption rate[51]

$$z=\frac{kT}{h}\bar{S}(T)\exp(-E_B/kT)\ . \tag{2}$$

Here $\bar{S}(T)\equiv\langle S(\mathbf{k},T)\rangle$ is a suitable average of the sticking coefficient $S(\mathbf{k},T)$ for Ps of momentum $\mathbf{k}$ incident upon the surface at temperature T from the vacuum. For decaying Ps atoms, the desorption rate is in competition with the annihilation rate γ of the surface Ps, leading to a thermal Ps desorption probability[52]

$$f_{\mathrm{Ps}}=z/(z+\gamma)\ . \tag{3}$$

The predicted energy spectrum of the perpendicular component of the emitted Ps kinetic energy $E_\perp$ should be a

beam Maxwell-Boltzmann distribution times the sticking coefficient $\bar{\bar{S}}(E_\perp,T)$, which has been averaged over the transverse components of the Ps velocity, i.e.,

$$dN/dE_\perp = \exp(-E_\perp/kT)\bar{\bar{S}}(E_\perp,T)/kT \ . \quad (4)$$

The sticking coefficient that appears in Eqs. (2)–(4) is connected with an interesting question: May the sticking coefficient $S_0 \equiv S(0,0)$ at low temperatures, and low Ps velocities have a value other than zero?[53–57] The value $S_0=0$ is expected due to the tendency of a quantum particle to reflect from a rigid potential. The conditions necessary for reaching the asymptotic limit where a measurement of $\bar{S}$ may be considered equivalent to a measurement of S_0 are not yet clear. One might expect that a Ps de Broglie wavelength of order 100 Å and a sample temperature of order 100 K would be sufficient. Nevertheless, sticking at zero velocity and temperature seems to require including the particle-surface interactions to high order, and a hand-waving argument may not be valid. With this in mind, we turn to the interpretation of our Ps thermal desorption measurements.

Our earlier experiments using a clean Al(111) sample have shown that the temperature dependence of f_{Ps} over the range $300\ \text{K} < T < 740\ \text{K}$ can be explained by Eqs. (2)–(4) if the value $\bar{S}=1$ is used.[8] Furthermore, a measurement of $dN/dE_\perp$ required $\bar{\bar{S}}(E_\perp,T)$ to be constant to within $\pm 10\%$ over the range $10\ \text{meV} < E_\perp < 200\ \text{meV}$ for $T=692$ K. An unconstrained fit to the data of Fig. 11 using Eqs. (2) and (3) (dotted curve) yields $E_B=(27\pm 7)$ meV and $\bar{S}=(2^{+2}_{-1})\times 10^{-3}$. If we constrain $\bar{S}\equiv 1$ (solid curve), the optimal binding energy is $E_B=100$ meV, but the fit is poor. Unlike the previous measurements on a clean Al(111) surface, however, it is possible that the O_2-exposed surface is not uniform, but contains patches of variable E_B. For example, we obtain a good fit to the areas of our time-of-flight curves by using the sum (dashed curve in Fig. 11) of two curves obtained from Eqs. (2) and (3) with $\bar{S}\equiv 1$ and $E_B\equiv 60$ and 120 meV with relative weights in the ratio 1:2. Alternately, if we allow there to be a background in Fig. 11, we would obtain a good fit to the data using $\bar{S}=1$ (long-dashed curve). However, there is probably no justification for such a background. The binding energies of about 100 meV are probably more reasonable than 27 meV, considering the clean Al value of 300 meV.

Since the energy distributions in Fig. 9 are simple exponential functions of $E_\perp$, we infer that $\bar{\bar{S}}(E_\perp,T)$ is a constant for $E_\perp$ between 5 and 50 meV for $84\ \text{K} < T < 284\ \text{K}$. If $\bar{\bar{S}}$ were proportional to $k_\perp$ for $E_\perp < 25$ meV and constant for $E_\perp > 25$ meV, by analogy with the internal e^+ reflectivity found in Ref. 14, then $dN/dE_\perp$ would be much smaller than observed at small values of $E_\perp$. Since the perpendicular projection of the Ps de Broglie wavelength is longer than 100 Å for much of the $(E_\perp,T)$ region explored, we have concluded in Ref. 24 that S_0 may be extrapolated from our measurements, and that therefore S_0 is not zero. Our previous result that gave $\bar{S}=1$ for clean Al, the plausibility of the dashed fit in Fig. 11, and recent theoretical work[58,59] suggest that $S_0=1$ is a definite possibility.

The measured Ps temperatures plotted in Fig. 10 are in agreement with the sample temperatures, and give further credence to the existence of a population of thermal Ps in vacuum from our low-temperature Al(111) samples. It is evident that we now have a source of cold Ps at temperatures as low as 150 K. The total intensity f_0 at 200 K is only about one-quarter of the Ps that may be obtained by heating a clean Al(111) sample to 690 K. However, for a Doppler-free measurement of the Ps $1S$-$2S$ interval,[17] the signal strength will be proportional to the amount of Ps at very low velocities, or f_0/kT. Thus, the signal strength using our cold Ps source should be the same as obtained using the higher temperature Ps, but the second-order Doppler shift, which includes contributions due to the transverse components of the Ps motion, would be about four times smaller.

V. CONCLUSION

We have examined the velocity distribution of the Ps emitted by Al(111) surfaces exposed to various amounts of oxygen at low temperatures. We find that the oxygen induces the emission of Ps with kinetic energies of a few tenths of an eV, in agreement with previous work. We also find that Ps is thermally desorbed at low temperatures and has a velocity distribution characterized by a temperature that is the same as that of the sample. The velocity distributions may be interpreted as indicating that the Ps has a sticking coefficient equal to 1 in the limit of zero velocity, unlike any other system studied to date.

[1] M. Deutsch, Phys. Rev. **82**, 455 (1951).
[2] K. F. Canter, A. P. Mills, Jr., and S. Berko, Phys. Rev. Lett. **33**, 7 (1974).
[3] For general reviews of the slow-positron method see A. P. Mills, Jr., in *Positron Solid State Physics,* edited by W. Brandt and A. Dupasquier (North-Holland, Amsterdam, 1983), p. 432; and P. J. Schultz and K. G. Lynn, Rev. Mod. Phys. **60**, 701 (1988).
[4] A. P. Mills, Jr., Phys. Rev. Lett. **41**, 1828 (1978).
[5] A. P. Mills, Jr. and L. Pfeiffer, Phys. Rev. Lett. **43**, 1961 (1979).
[6] K. G. Lynn, Phys. Rev. Lett. **43**, 391 (1979); **43**, 803 (1979).
[7] A. P. Mills, Jr., Solid State Commun. **31**, 623 (1979).
[8] A. P. Mills, Jr. and L. Pfeiffer, Phys. Rev. B **32**, 53 (1985).
[9] A. P. Mills, Jr., L. Pfeiffer, and P. M. Platzman, Phys. Rev. Lett. **51**, 1085 (1983).

[10]P. Sferlazzo *et al.*, Phys. Rev. Lett. **60**, 538 (1988).
[11]A. P. Mills, Jr., E. D. Shaw, R. J. Chichester, and D. M. Zuckerman, Phys. Rev. B **40**, 8616 (1989).
[12]R. H. Howell, P. Meyer, I. J. Rosenberg, and M. J. Fluss, Phys. Rev. Lett. **54**, 1698 (1985).
[13]K. G. Lynn *et al.*, Phys. Rev. Lett. **54**, 1702 (1985).
[14]D. M. Chen *et al.*, Phys. Rev. Lett. **58**, 921 (1987).
[15]R. H. Howell *et al.*, Phys. Rev. B **35**, 5303 (1987).
[16]R. H. Howell, I. J. Rosenberg, P. Meyer, and M. J. Fluss, Phys. Rev. B **35**, 4555 (1987).
[17]S. Chu, A. P. Mills, Jr., and J. L. Hall, Phys. Rev. Lett. **52**, 1689 (1984).
[18]K. G. Lynn and H. Lutz, Phys. Rev. B **22**, 4143 (1980).
[19]K. G. Lynn and H. Lutz, Rev. Sci. Instrum. **51**, 977 (1980).
[20]K. G. Lynn, Phys. Rev. Lett. **44**, 1330 (1980).
[21]Y. C. Jean, K. G. Lynn, and M. Carroll, Phys. Rev. B **21**, 4935 (1980).
[22]I. J. Rosenberg, A. H. Weiss, and K. F. Canter, J. Vac. Sci. Technol. **17**, 253 (1980).
[23]R. J. Wilson and A. P. Mills, Jr., Phys. Rev. B **27**, 3949 (1983).
[24]A. P. Mills, Jr. *et al.*, Phys. Rev. Lett. **66**, 735 (1991).
[25]A. P. Mills, Jr., P. M. Platzman, and B. L. Brown, Phys. Rev. Lett. **41**, 1076 (1978).
[26]B. Nielsen, K. G. Lynn, and Y. C. Chen, Phys. Rev. Lett. **57**, 1789 (1986).
[27]R. H. Howell, I. J. Rosenberg, and M. J. Fluss, Phys. Rev. B **34**, 3069 (1986).
[28]D. T. Britton, P. A. Huttunen, J. Mäkinen, E. Soininen, and A. Vehanen, Phys. Rev. Lett. **62**, 2413 (1989).
[29]C. H. Hodges and M. J. Stott, Solid State Commun. **12**, 1153 (1973).
[30]R. Paulin, R. Ripon, and W. Brandt, Phys. Rev. Lett. **31**, 1214 (1973).
[31]R. Nieminen and M. Manninen, Solid State Commun. **15**, 403 (1974).
[32]P. M. Platzman and N. Tzoar, Phys. Rev. B **33**, 5900 (1986).
[33]D. W. Gidley, A. R. Köymen, and T. W. Capehart, Phys. Rev. B **37**, 2465 (1988).
[34]K. G. Lynn, Phys. Rev. Lett. **44**, 1330 (1980).
[35]R. Mayer and K. G. Lynn, Phys. Rev. B **33**, 3507 (1986).
[36]J. E. Crowell, J. G. Chen, and J. T. Yates, Surf. Sci. **165**, 37 (1986).
[37]J. G. Chen, J. E. Crowell, and J. T. Yates, Phys. Rev. B **33**, 1436 (1986).
[38]D. M. Chen *et al.*, Phys. Rev. B **39**, 3966 (1989).
[39]R. H. Howell, R. A. Alverez, and M. Stanek, Appl. Phys. Lett. **40**, 751 (1982).
[40]A. P. Mills, Jr., E. D. Shaw, R. J. Chichester, and D. M. Zuckerman, Rev. Sci. Instrum. **60**, 825 (1989).
[41]D. W. Gidley, P. W. Zitzewitz, K. A. Marko, and A. Rich, Phys. Rev. Lett. **37**, 729 (1976).
[42]A. P. Mills, Jr., E. D. Shaw, R. J. Chichester, and D. M. Zuckerman, Phys. Rev. B **40**, 2045 (1989).
[43]R. H. Howell, M. Tuomisaari, and Y. C. Jean, Phys. Rev. B **42**, 6921 (1990).
[44]D. M. Bylander, L. Kleinman, and K. Mednick, Phys. Rev. Lett. **48**, 1544 (1982).
[45]I. P. Batra and L. Kleinman, J. Electron Spectrosc. Relat. Phenom. **33**, 175 (1984).
[46]D. S. Wang and A. J. Freeman, Phys. Rev. B **19**, 4930 (1979).
[47]H. Krakauer, M. Posternak, A. J. Freeman, and D. D. Koelling, Phys. Rev. B **23**, 3859 (1981).
[48]D. S. Wang, A. J. Freeman, and H. Krakauer, Phys. Rev. B **24**, 3092 (1981); **24**, 3104 (1981); **24**, 3614 (1981).
[49]J. L. Erskine and R. L. Strong, Phys. Rev. B **25**, 5547 (1982).
[50]C. F. McConville, D. L. Seymour, D. P. Woodruff, and S. Bao, Surf. Sci. **188**, 1 (1987).
[51]J. E. Lennard-Jones *et al.*, Proc. R. Soc. London, Ser. A **156**, 6 (1936); **156**, 36 (1936).
[52]S. Chu, A. P. Mills, Jr., and C. A. Murray, Phys. Rev. B **23**, 2060 (1981).
[53]G. Iche and P. Nozières, J. Phys. (Paris) **37**, 1313 (1976).
[54]T. R. Knowles and H. Suhl, Phys. Rev. Lett. **39**, 1417 (1977).
[55]G. Doyen, Phys. Rev. B **22**, 497 (1980).
[56]K. Schönhammer and O. Gunnarsson, Phys. Rev. B **22**, 1629 (1980).
[57]T. Martin, R. Bruinsma, and P. M. Platzman, Phys. Rev. B **38**, 2257 (1988).
[58]T. Martin, R. Bruinsma, and P. M. Platzman, Phys. Rev. B **39**, 12 411 (1989).
[59]T. Martin and R. Bruinsma, Phys. Rev. B **41**, 3172 (1990).